CHAPTER 2

LITERATURE REVIEW

2.1 Introduction

This chapter includes a brief literature survey on the possible capability of zirconia and alumina-based ceramics (3Y-TZP, 8Mg-PSZ, and ZTA) and their composites with bioactive glass in dental and orthopedic applications. The 3Y-TZP, 8Mg-PSZ, and ZTA have been used as biomaterials for a long time. Martin Heinrich Klaproth introduced zirconia, or zirconium oxide, in 1789 (Raigrodski *et al.*, 2004). This substance is a noncytotoxic metal oxide that is not soluble in water and cannot adhere to bacteria. It also offers minimal corrosion characteristics (Dion *et al.*, 1994) (Scotti *et al.*, 2007). Until now, zirconia has been regarded as an excellent option for dental restorations because of its low plaque, tooth-colored look, and good mechanical qualities (Olsson *et al.*, 2003) (Bremer *et al.*, 2011) (Bateli *et al.*, 2014). Notably, reports of using alumina as a porous bone substitute and dental implant date back to the early 1960s (Al-Moameri *et al.*, 2020). Because of its strong chemical inertness, both of these ceramics are highly biologically safe, even at higher specific surfaces. Alumina and zirconia, whose hardness is higher than that of other metal alloys, are primarily used as biomaterials in the articular surfaces of joint replacements (Žmak *et al.*, 2019). Zirconia ball heads are essentially no longer used in hip arthroplasty procedures today. While zirconia ceramics are still utilized in some specialized orthopedic goods, its primary application is in dentistry. Zirconia is utilized with alumina in ceramic composites, which are currently the standard bioinert ceramic for clinical applications (He *et al.*, 2008).

This chapter provides a brief description of the possible synthesis process for different matrix ceramics and reinforcement materials. It also explains how bioactive glass (BG) is added to bioinert ceramics to make bioactive ceramics. It also examines the impact of BG on the mechanical, biological, and structural properties of ceramics. In order to comprehend current developments in implant materials and non-traditional machining of implant materials, this chapter also clarifies the studies involved in the field of machining for implant

materials, particularly in biomedical industries. At last tribological behaviour of composite materials is also discussed. A summary of the research that has been done is provided, along with a detailed description of how the current biocomposite materials behave.

2.2 Synthesis of matrix ceramics (3Y-TZP, 8Mg-PSZ, and ZTA)

To date, the 3Y-TZP have been synthesized by several synthetic strategies such as solvothermal, hydrothermal, organic precursor route, aqueous synthesis, co-precipitation, homogeneous precipitation, sol-gel, spray drying, flame spray pyrolysis, plasma spray, molecular decomposition, spray-ICP, and auto-combustion methods (Biswas *et al.*, 2011) (Rao *et al.*, 1995). For the synthesis of Mg-PSZ, numerous techniques have been put forth, including a traditional solid-state reaction (Li *et al.*, 2013) (Deng *et al.*, 2019), precipitation and co-precipitation techniques (Kong *et al.*, 2012) (Yamagata *et al.*, 2015) (Prochazka *et al.*, 2014), a polymeric precursor route (Aytimur *et al.*, 2012), sol-gel processing (Nakonieczny *et al.*, 2014) (Judes *et al.*, 2014) (Keerthana *et al.*, 2019) (Mirtaleb *et al.*, 2019), pechini method (Keerthana *et al.*, 2019) (Hajizadeh-Oghaz *et al.*, 2015), sugar technique (Septawendar *et al.*, 2012), plasma spray synthesis (Keerthana *et al.*, 2019) (Buyakova *et al.*, 2016), electrospinning (Heuer *et al.*, 2020), auto-combustion (Biswas *et al.*, 2011) and microwave heating technique (Chen *et al.*, 2021). Several powder synthesis techniques, including dry milling (Kibbel *et al.*, 1986), wet milling (Tahmasebi *et al.*, 2011), co-precipitation (Peng *et al.*, 2000) (Ramanathan *et al.*, 1996), sol-gel (Kureti *et al.*, 2002) (Hong *et al.*, 1995), and auto-combustion (Biswas *et al.*, 2011) have been explored for the synthesis of ZTA nano-ceramics.

Auto-combustion is among the most effective methods for synthesizing nanopowder. Initiated with the help of an external heating source, this process starts at a low temperature and progresses to an exothermic reaction between the fuel and oxidizer. The heat generated

propels the reaction forward, resulting in the formation of nanocrystalline powders. Various organic fuels have been tested for producing nano-ceramic powders, including urea, sucrose, oxalyl dihydrazide, glycine, urea-formaldehyde, and glycine nitrate. (Mukasyan *et al.*, 2001) (Chavan *et al.*, 2004) (Aruna *et al.*, 1997) (Prabhakaran *et al.*, 2007) (Biswas *et al.*, 2007).

2.3 Synthesis of reinforcement material (bioactive glass)

The two main methods used to produce bioactive glass powders are sol-gel and melt quench. The melt-quench method involves melting the elements of the bioactive glasses in precise quantities to yield the desired composition. The molten liquid is quickly cooled or quenched, and crushed to powder. This quenching can be done with either water or liquid nitrogen. Furthermore, glass powder can be manufactured by collecting and milling granules of varying sizes, known as frits. Molten glass can be poured into molds of precise diameters to get the required shape and scale. This technology is adaptable and can be used to make a variety of bioactive glasses (Karasu *et al.*, 2019).

In contrast, the sol-gel approach is a wet chemical reaction that takes place at low temperatures. In this process, a solution containing the necessary precursors in the needed proportions undergoes hydrolysis and polycondensation reactions at room temperature to generate the gel. The gel is subsequently dried and heated to form the amorphous glass architecture. The sol is poured into petri dishes to produce gels, and then the bonds are strengthened through aging. Finally, the gel is dried out and ground into glass powder (Yadav *et al.*, 2020). Fig. 2.1 shows a schematic flow chart of melting and sol-gel techniques for the synthesis of bioactive glasses.

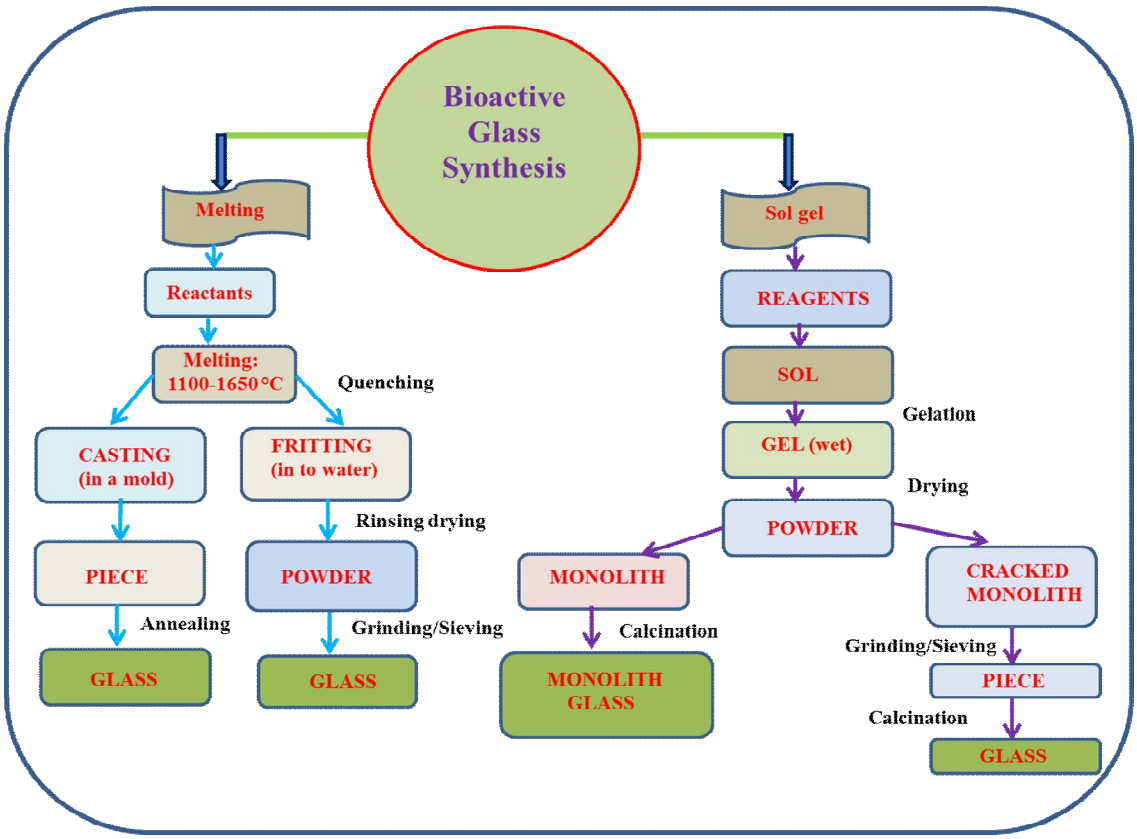

Fig. 2.1 A schematic flow chart of different techniques for the synthesis of bioactive glasses. (Reproduced with permission from (Kaur *et al.*, 2016)).

2.4 Stimulating bone growth

In order to promote bone growth in bio-inert materials, bioactive glass first causes the formation of hydroxy carbonate apatite (HCA) by precipitation and dissolution. Next, the HCA layer interacts with the weak collagen fibrils to form a connection with the bone. The products of degradation stimulate cells throughout the process. HCA making happens in five steps, comparable to normal glass corrosion mechanisms (Jones *et al.*, 2013).

- Rapid cation exchange (Na^+, K^+, Mg^{+2}, and Ca^{+2}) in glass interacts with H^+ from the solution to generate silanol linkages (Si-OH) on its surface. This elevates the local pH, which leads to the development of a silica-rich zone around the glass surface. (If phosphate is included in the glass composition, it is also released during the first stage.)

- As the pH rises, OH^- ions engage with the silica glass network, breaking the Si-O-Si bonds and forming $Si(OH)_4$, resulting in the production of Si-OH (silanol) at the glass-solution interface.
- Si-OH groups concentrate along the glass surface in the silica-rich layer.
- An amorphous $CaO–P_2O_5$ layer is formed when Ca^{+2} and $PO4^{-3}$ groups move from the solution and bulk glass to the silica-rich layer's surface.
- HCA (the mineral phase of teeth and bone) develops in-situ when hydroxyls and carbonate ions from solution crystallize and combine with $CaO–P_2O_5$. This composition attaches to soft tissue as well as bone and teeth (Jones *et al.*, 2013) (O'Donnell, 2012).

Fig. 2.2 depicts a schematic representation of hydroxycarbonate apatite (HCA) output on the surface of bioactive glass. First, silanol bonds (Si-OH) are formed on the glass surface; next, the pH of the solution is raised to encourage the formation of a silica-rich area near the glass surface; third, silica bonds break down; fourth, additional silanol is formed at the glass–solution interface; fifth, a silica-rich layer precipitates; sixth, an amorphous $CaO–P_2O_5$ layer forms on the formed silica-rich layer; and seventh, the amorphous $CaO–P_2O_5$ layer crystallizes into apatite (Henao *et al.*, 2019).

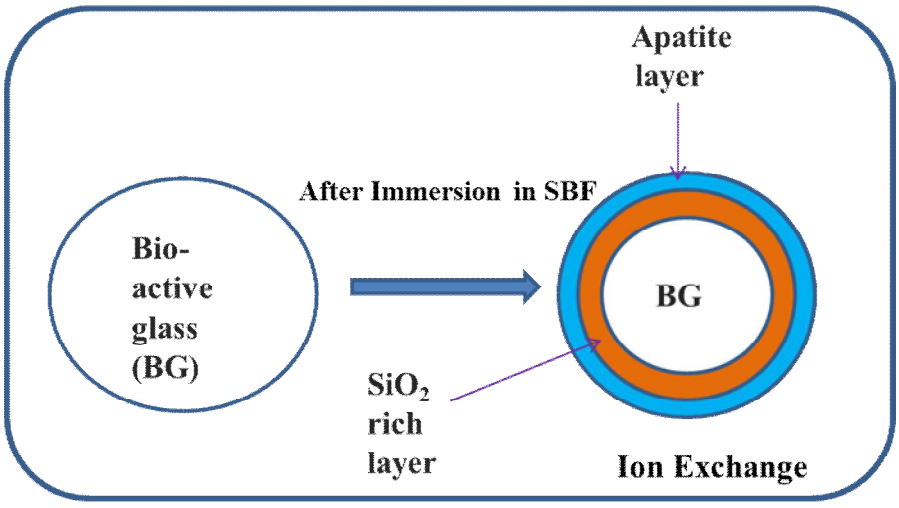

Fig. 2.2 Schematic representation of the dissolution behavior of silicate bioactive glasses in simulated body fluid (Henao *et al.*, 2019).

The apatite layer production and bone growth surrounding the implant are influenced by the nature of the bioactive glass. A less connected network is linked to bioactive glass with a low silica content. This accelerates the development of apatite and encourages the dissolution of bioactive glass. Bioactivity and the activation energy of silica dissolution in glasses are frequently linked. However, the quantity of silica in glass and the connectedness of the glass network affect their bioactivity. While cations like sodium and calcium speed up the rate of dissolution and boost bioactivity, multivalent ions like Al^{+3} or Ti^{+4} in bioactive glass decrease bioactivity and solubility (Aparicio *et al.*, 2015). Because of their strongly linked network, glasses with a high silica content have decreased bioactivity and dissolution. Therefore, for bioactivity and dissolution, network modifiers with the ability to weaken the glass network are crucial. Bioactive glasses are perfect for cell attachment and proliferation because they can interact with the physiological environment to trigger in vivo osteogenesis on the implant surface (Henao *et al.*, 2019).

2.5 Enhancement of *in-vitro* bioactivity

The primary disadvantage of the zirconia and alumina-based ceramics (3Y-TZP, Mg-PSZ, and ZTA) is their biologically inertness behavior, despite their good mechanical and biocompatibility (Hao *et al.*, 2005). The fibrous fibers surround the implant and prevent osseointegration, no chemical linkages are formed between the implant and the surrounding bone tissues. The process of osseointegration is essential to the success of an implant because it promotes bone repair and the creation of new bone (Viceconti *et al.*, 2000). It is well known that, a bioactive material can develop a strong link with living bone by the formation of an apatite layer on its surface. The micro-arc oxidation of zirconium, CO_2-irradiation (Yan *et al.*, 2007), chemical etching (Hao *et al.*, 2004), ion implantation (Uchida *et al.*, 2002), surface coating (Liang *et al.*, 2007), Al_2O_3 cyclone sandblasting (Kim *et al.*, 2004)

(Sandhyarani *et al.*, 2014), dopamine modification (Yamashita *et al.*, 2009), biomimetic mineralization (Zain *et al.*, 2014), and incorporation of bioactive materials such as calcium phosphate, bioactive glass, and wollastonite (Stefanic *et al.*, 2012) are different techniques through which the bioinert material can achieve good surface bioactivity. A range of surface modification techniques applied to bio-inert ceramics have been evaluated scientifically to enhance their adherence (Liu *et al.*, 2014) (Matinlinna *et al.*, 2018). These surface modifications may have an impact on the biological interfacial characteristics. The Merriam-Webster Dictionary defines "an interface" as "a surface forming a common boundary of two bodies, spaces, or phases". An interface, or border between two bodies, would be formed by the surfaces of the two things. Therefore, a surface treatment may alter the interfacial surface properties, which are crucial for bio-inert ceramic's biological performance as well.

2.6 Cell adhesion

Cell adhesion is intimately related to the processes of cell differentiation and proliferation that follow. It significantly affects the integration of biomaterials and tissues. On a material surface, protein adsorption is thought to be the initial stage of cell attachment (Luo *et al.*, 2018) (Anselme *et al.*, 2020). The surface properties play a crucial role in the interface between the material and the cell, as they can control different intracellular signal connections related to cell adhesion, proliferation, and differentiation (Ku *et al.*, 2010) (Docheva *et al.*, 2007) (Hallab *et al.*, 2001). However, the impact of surface features on cell attachment and proliferation, such as surface roughness, surface chemistry, surface free energy (SFE), and has been extensively studied in dentistry research (Anselme *et al.*, 2000) (Kim *et al.*, 2015) (Lim *et al.*, 2004).

Determining the impact of surface roughness on cell responsiveness is essential to comprehending and enhancing the effectiveness of implant materials. It is commonly known

that, in comparison to smooth implant surfaces, materials having a moderately high surface roughness may accelerate early cell attachment (Yamashita *et al.*, 2009) (Deligianni *et al.*, 2000) (Huang *et al.*, 2004) (Deligianni *et al.*, 2001). One possible explanation is that the roughness gradient leads to significant differences in solidity, aspect ratio, and cell area. The micro-roughness factors seem to be nonlinearly related to cell area, whereas, nano-roughness variables are found to be linearly related to cell solidity. This suggests that multiscale optimization of implant surface roughness and topography is crucial to eliciting the optimal cell response (Flamant *et al.*, 2016). It has been shown that the formation of micro-grooves on a rough surface can alter the shape of human embryonic osteoblasts and direct their size and alignment. Zirconia surfaces with 30 μm wide microgrooves spaced 70 μm apart have been shown to boost alizarin red (ALZ) and alkaline phosphatase (ALP) synthesis in human embryonic osteoblasts (Delgado-Ruíz *et al.*, 2016). Another phenomenon that has been observed is that the human fetal osteoblastic cell line (hFOB) can have its bioactivity, such as cell proliferation and ALP activity. It is increased when it is exposed to a nano-patterned surface with arrays of nano-scale islets compared to control substrates (Soon *et al.*, 2017).

Several surface treatments, such as the addition of distinct chemical ions, can alter the surface chemistry (Schafer *et al.*, 1991), and coatings (Lung *et al.*, 2010) (Lung *et al.*, 2015) (Matinlinna *et al.*, 2013). Certain chemical modifications applied to bioceramics may lead to alterations in the material's biological interfacial performance. The goal of adding certain chemical ingredients is to enhance its biological properties. After firing the zirconia surface, calcium ions are added (with calcium acetate) to create $CaZrO_3$, which enhances the SFE of the material and shows good initial cell attachment to the material (Sasaki *et al.*, 2015). On Ca-P (calcium phosphate) spots on modified zirconia, MC3T3-E1 osteoblast cells are attached and proliferate more readily (Kozelskaya *et al.*, 2018). Mesenchymal stem cells adhere to the tribasic calcium phosphate coating more readily in zirconia substrate coated

with calcium phosphate than uncoated (Hadjicharalambous *et al.*, 2015). Magnesium ions have also been used in addition to calcium and phosphate to alter the biological characteristics. The ALP activity and collagen deposition of MC3T3-E1 pre-osteoblast cells are significantly higher in magnesia-stabilized porous zirconia substrate coated with mineralized calcium compared to magnesia-stabilized porous zirconia. It is demonstrated that pre-osteoblasts may be guided into a mature state capable of mineralizing the extracellular matrix by magnesia-stabilized porous zirconia (Pardun *et al.*, 2015). The impact of adding magnesium to zirconia-calcium phosphate coatings is also examined. It is found that the Mg-containing coatings are outperformed pure zirconia-calcium phosphate coatings in terms of human osteoblast cell proliferation and differentiation (Altmann *et al.*, 2017).

To enhance zirconia's biological characteristics, a thin layer of HA is added (Saito *et al.*, 2014). It is observed that on the HA films modified zirconia, there is an increase in the osteoblast cell's ALP activity and bone formation area (Pae *et al.*, 2014). In a different investigation, the osteoblast cell adhesion and proliferation are outperformed with hydroxyapatite-based plasma electrolytic coatings on the zirconia compared to without coating (Ozeki *et al.*, 2014). Compared to uncoated zirconia, specimens coated with micro-patterned silica thin films (MSTF) and nano-HA are found to exhibit increased cell metabolic activity and proliferation after 7 days of culture (Aktuğ *et al.*, 2017).

The coating with bioactive glass also improves the bioactivity in bio-inert materials. An apatite layer is developed on the surface of zirconia coated with BG when submerged in the simulated bodily fluid (SBF). Compared to (control) untreated zirconia substrate, the growth of fibroblasts and osteoblast-like cells on bioactive glass-covered zirconia shows a greater proliferation rate, higher cell density, and higher expression of ALP activity (Bosetti *et al.*, 2021). It is also shown that the bioactive glass-coated zirconia increases the osseointegration of zirconia ceramics in the animal model compared to uncoated zirconia,

(Stanic *et al.*, 2002). Recently, bioactive glass has been applied to the zirconia surface layers using grain-boundary activation. It entails the gelling and sintering procedures after a bioactive glass sol is introduced into the un-sintered zirconia grain boundary surfaces. The cultivation of mesenchymal stem cells (mBMSCs) generated from mouse bone marrow reveals that the bioactive surface modification of zirconia may promote cell adhesion and differentiation. In the future, this bioactive glass may be revolutionary for dental implants (Ke *et al.*, 2017).

2.7 Bacterial adhesion

An outline of some surface properties' implications on cell adhesion to bioceramic materials has been provided above. Having said that, it should come as no surprise that the physical and chemical properties of the material surface are linked to the microbial colonizers' adherence to dental materials (An *et al.*, 1998) (Katsikogianni *et al.*, 2004). It is known that surface properties significantly affect the adherence of bacteria. This specifically pertains to surface chemistry, SFE, and surface roughness (Katsikogianni *et al.*, 2004) (Quirynen *et al.*, 1995) (Hämmerle *et al.*, 2009).

Regardless of the implant material, it has been determined that biofilm production and maturation are rising on the dental implant surface with larger surface roughness (Teughels *et al.*, 2006). Remarkably, when the roughness is decreased, that is, when the Ra value is lower than 0.2 μm, the biofilms do not considerably diminish, indicating that 0.2 μm is intended to be "the threshold Ra" (Bollen *et al.*, 1996) (Quirynen *et al.*, 1996). In a recent investigation, the impact of surface roughness on Streptococcus mutans's (S. mutans) adherence and biofilm formation on zirconia is investigated. It has been found that the adhesion force and early attachment (2 and 4 hrs) of S. mutans on the zirconia may be influenced by the surface roughness (Ra) at the nanoscale. Nevertheless, it has little effect on biofilm formation later on

(6, 8, 12, and 24 hrs) (Yu *et al.*, 2016). However, there is disagreement over how surface roughness affects the activity of bacteria on zirconia. In a prior investigation, differences in zirconia's surface roughness has no effect on Staphylococcus epidermidis adherence. A surface with a higher Ra generally displays greater adherence to Streptococcus sanguinis. It is observed that while surface roughness might affect how well bacteria adhere to zirconia, the majority of influencing factors are the types of bacteria (Wassmann *et al.*, 2017). The measurement and criteria for roughness are "very confusing and lack unity," indicating that various implant studies use different standards for surface roughness (Matinlinna *et al.*, 2013).

Electrostatic interactions between bacteria and the chemical makeup of material surfaces directly affect the capacity of bacteria to attach to surfaces and form a biofilm. In light of this, zirconia's chemical composition has also changed to enhance its biological interfacial performance. Numerous studies have looked into how to stop bacteria from adhering to zirconia and from forming biofilms. According to a study, zirconia coated with nanocrystalline silver can release Ag+ as well as free silver, Ag0, which reduces postoperative infections (Pérez-Tanoira *et al.*, 2016). It has been discovered that zirconia coated with glass ceramic powder (which contains Ag and F) decreases S. mutans' adherence (Oh *et al.*, 2019). Strong bactericidal effects of immobilized silver nanoparticles (AgNano) on zirconia have been demonstrated by the elimination of residual microorganisms (Wehling *et al.*, 2015). The bactericidal action of Ag-nanoparticle-coated zirconia is not mediated by the liberated Ag+ ions but rather corresponds to contact killing, according to the understood underlying mechanism of its antibacterial activity (Yamada *et al.*, 2017). Bioactive glass generally improves the in vitro bioactivity, cellular viability, and antibacterial response of ceramics based on zirconia. Incorporating bioactive glass serves as a sintering additive in addition to enhancing biological response. Since solid-state sintering is typically used to

create zirconia-based ceramics at temperatures between 1500 and 1600 °C, the goal is to lower the sintering temperature and, consequently, the manufacturing costs (Stevens, 1986).

2.8 Addition of different bioactive glass into various zirconia-based bioceramic composites

Zirconia-based bioceramics such as 3Y-TZP (3 mol% yttria-stabilized tetragonal zirconia polycrystals), 8Mg-PSZ (8 mol% magnesia-partially stabilized zirconia), and ZTA (zirconia-toughened alumina) are prominent materials used in implant applications. Their unique combinations of mechanical strength, fracture toughness, wear resistance, and biocompatibility make them ideal for various medical devices. The addition of bioactive glass to bioceramics such as 3Y-TZP, 8Mg-PSZ, and ZTA enhances their properties, particularly in terms of bioactivity, osteointegration, and overall performance in medical implants. These improvements lead to better integration with bone tissue, faster healing times, and increased stability and longevity of the implants.

2.8.1 Yttria-stabilized tetragonal zirconia polycrystals (Y-TZP)

Yttrium stabilized TZP (Y-TZP) has garnered attention as a promising material for implants due to its exceptional mechanical qualities, favorable biocompatibility, and unique visual appeal. Y-TZP's biological inertness, on the other hand, prevents it from forming chemical bonds with bone tissue, which compromises the stability and long-term effectiveness of Y-TZP implants. Soubelet *et al.* (Soubelet *et al.*, 2024) have synthesized zirconia-based composites with 2.5, 5, and 10% addition of 64S bioactive glass (BG). The inclusion of 64S glass not only enhances biocompatibility but also improves the Vickers hardness values by approximately 13 GPa. He *et al.* (He *et al.*, 2023) have mixed different 58S, 68S, and 77S bioactive glass in Y-TZP ceramic. The modified Y-TZP/BG samples have

increased bioactivity, which is mainly demonstrated by their increased capacity for protein adsorption and their ability to release osteogenic-related ions into the culture medium over an extended period without significantly changing the pH. Additionally, cells grown on Y-TZP samples show improved osteogenic differentiation, adhesion, spreading, vitality, and proliferation. Yun *et al.* (Yun *et al.*, 2023) have altered the 3Y-TZP surface by adding a biocomposite of hydroxyapatite and forsterite. The surface modification with a hydroxyapatite and forsterite biocomposite has improved the bioactivity of the 3Y-TZP substrate in SBF solution. Zhang *et al.* (Zhang *et al.*, 2022) have modified Y-TZP ceramics through grain-boundary activation by coating the crystal surfaces of zirconia powder with a variable quantity of bioactive glass (BG) sol. The *in-vitro* mineralization results demonstrate that after the Y-TZP ceramics are submerged in the SBF for 21 days, a homogenous apatite layer is formed on the surface. The results of the cell response suggest that Y-TZP ceramics' bioactive surface modification enhances cell adhesion, propagation, and osteogenic differentiation capacity. Fabris *et al.* (Fabris *et al.*, 2021) have infused S53P4 bioglass into zirconia disks. The infiltration of BG into a zirconia structure produced a layer around 100 μm thick BG coating. The BG coating reduces 30% implant body stress. de Oliveira *et al.* (de Oliveira *et al.*, 2021) have created porous ceramic based on 5 mol.% yttria stabilized zirconia (5Y-PSZ) with 45S5 bioactive glasses suitable for the infiltration using 3D-printed sacrificial polymeric molds. The 45S5 bioactive glass, calcium sodium phosphor-silicate, is infiltrated into the porous 5Y-PSZ ceramics. Awalia *et al.* (Awalia *et al.*, 2020) have investigated the flexural strength of yttria-stabilized zirconia (Y-TZP) coated with CO3Ap as a dental implant material. It is found that the coating with CO_3Ap does not affect its mean flexural strength. Soubelet *et al.* (Soubelet *et al.*, 2019) have synthesized 3 mol-% yttria-partially stabilized zirconia (Y-TZP) with 5.4, 10.5, and 19.9 vol.-% 64S bioglass and sintered at temperatures ranging from 1300°C to 1500°C. The maximum hardness and flexural strength are observed

in Y-TZP containing 10.5 vol.-% 64S at 1400°C, making it the most promising ceramic in terms of mechanical properties and aging resistance. de Paula Miranda *et al.* have incorporated bioactive glasses into a Y: TZP matrix to enhance the bioactivity and osseointegration of this material. The addition of BG leads to a decrease in its relative density and flexural strength (de Paula Miranda *et al.*, 2019). Ke *et al.* have studied the grain-boundary activation by infiltrating a bioactive glass sol into the surface layers of Y-TZP ceramics under different pressures (atmospheric pressure, −0.05 kPa, and −0.1 kPa), followed by gelling and sintering. Bioactivity tests are conducted by immersing Y-TZP in simulated body fluid (SBF) and it is revealed that a bonelike apatite layer is formed on the entire surface. However, samples, infiltrated with BG sol at −0.05 kPa, and atmospheric pressure, maintain good mechanical performance. Cell culture results indicate that the bioactive surface modification of Y-TZP enhances cell adhesion and differentiation (Ke *et al.*, 2017). Sun *et al.* have examined a graded glass/graded zirconia (G/Z) system synthesized by infiltrating a low-modulus nanosized glass into a zirconia surface. Cell viability tests indicate that no significant decrease in G/Z- and Y-TZP-treated cells over 72 hours. Fluorescence and SEM images show similar cell spreading on Y-TZP and G/Z, with cells appearing flattened and well-spread. Cellular toxicity results show no significant difference in LDH release for G/Z compared to Y-TZP over 72 hours. There are no significant changes in cell cycle distribution for cells cultured with G/Z compared to those cultured with Y-TZP or the untreated control group. No apoptosis is observed in cells cultured with Y-TZP and G/Z compared to untreated controls at 24 and 48 hours (Sun *et al.*, 2017). Brook *et al.* have examined the biological response of strontium (Sr)-doped hydroxyapatite (HA) and hydroxyapatite–zirconia (HA–ZrO_2) composites produced using sol-gel technology. *In-vitro* evaluations demonstrate that all materials elicit a favorable response from rat osteosarcoma cells. *In-vivo* assessments reveal osteoconductivity and biocompatibility for both Sr–HA and HA–ZrO_2, with no

inflammatory responses in bone. The Sr–HA composite shows superior biocompatibility, likely due to the incorporation of Sr and the formation of a surface apatite layer (Brook *et al.*, 2012). Lin *et al.* have created porous zirconia scaffolds by infiltrating acrylonitrile butadiene styrene (ABS) scaffolds with a 3 mol% yttria-stabilized zirconia slurry. Following sintering, a sol-gel dip coating method is applied to add a layer of mesoporous bioglass (MBGs). The average thickness of the coating layer was approximately 7 μm. The uncoated porous zirconia demonstrates high porosity levels, ranging from 60.1% to 63.8%, with most macropores, approximately 0.5-0.8 mm in size, being interconnected. These scaffolds have compressive strengths between 9.07 and 9.90 MPa. Bone marrow stromal cell (BMSC) proliferation tests indicate good biocompatibility for both coated and uncoated zirconia scaffolds. Scanning Electron Microscope (SEM) images and compositional analysis reveal apatite formation on the coating surface after immersion in simulated body fluid (SBF) for 7 days. The modification of porous zirconia-based ceramics with a bioactive mesoporous bioglass coating shows promise for potential biomedical applications (Lin *et al.*, 2011). Ho *et al.* have investigated the impact of glass frits on the sintering and mechanical properties of dental 3Y-TZP ceramics. The glass frits, composed of MgO, CaO, Al_2O_3, SiO_2, and P_2O_5, are chosen to reduce the sintering temperature of zirconia through liquid phase sintering. The addition of glass frits is found to significantly influence both the mechanical properties and relative densities of the ceramics. At lower sintering temperatures, the presence of glass additives enhances the mechanical properties, while at higher sintering temperatures, they lead to a decrease in mechanical properties (Ho *et al.*, 2011). Bicalho *et al.* have explored the cyclic fatigue life of 3 mol% Y_2O_3-stabilized ZrO_2 (3Y-TZP) ceramics doped with bioactive glass. The cyclic fatigue life is assessed using four-point bending tests at a frequency of 25 Hz and a stress ratio of 0.1. After sintering, the highly dense tetragonal ZrO_2 samples show hardness values of 10.5 and 11 GPa, KIC values of 6 and 7 $MPam^{1/2}$, bending strengths of 320 and 450

MPa, and Weibull moduli of 6 and 7 for samples containing 5% and 3% bioglass, respectively. The fatigue behavior shows that an increase in stress levels leads to a decrease in the number of cycles and run-out specimens. Samples containing 3% bioglass are approximately 10% more resistant to fatigue, exhibiting a cyclic fatigue life near 250 MPa, whereas samples with 5% bioglass had a fatigue limit near 220 MPa (Bicalho *et al.*, 2010) . Habibe *et al.* have studied 3Y-TZP ceramics with varying bioglass additions (0 to 30 wt.%) that are cold uniaxially pressed at 80 MPa and sintered in air at either 1200°C or 1300°C for 120 minutes. The results indicate that increasing the bioglass content leads to a decrease in relative density, attributed to martensitic (tetragonal to monoclinic) transformation during the cooling of the sintered samples. Y-TZP samples sintered at 1300°C with 5 wt.% bioglass shows the best results, achieving high relative density, hardness, and fracture toughness of 11.3 GPa and 6.1 $MPam^{1/2}$, respectively (Habibe *et al.*, 2009). Santos *et al.* have studied ZrO_2–bioglass ceramics by blending 3 mol% Y_2O_3-stabilized ZrO_2 with varying amounts of bioglass from the $3CaO•P_2O_5–MgO–SiO_2$ system. The findings indicate that ceramics sintered at 1300°C with a 3% bioglass addition exhibit the highest strength of 435 MPa, hardness of 1170 HV, and fracture toughness of 6.3 $MPam^{1/2}$(Santos *et al.*, 2008). Kishi *et al.* have created a composite ceramic of nano-sized hydroxyapatite doped zirconia (nanoHAP-Z) with a minimal amount of HA. Scanning electron microscopy reveals the formation of a bone-like apatite layer that completely covers the surface of nanoHA-Z ceramics when immersed in simulated body fluid (SBF). This enhanced apatite formation is attributed to an increase in the concentrations of Ca and PO_4. The utilization of the Chemicovector effect is demonstrated as a potent method for enhancing biomaterials (Kishi *et al.*, 2006). (Nogiwa-Valdez *et al.* have synthesized zirconia-alumina composites with $CaO-SiO_2$ glass (wollastonite). To enhance bioactivity, the composites undergo biomimetic treatment.

Following 21 days of immersion in simulated body fluid (SBF), a bone-like apatite layer is formed (Nogiwa-Valdez *et al.*, 2006).

2.8.2 8-mol% Magnesia-partially stabilized zirconia (Mg-PSZ)

Magnesium-stabilized partially stabilized zirconia (Mg-PSZ) has garnered significant attention as a promising material for implants due to its exceptional combination of mechanical properties, biocompatibility, and corrosion resistance. The stabilization provided by magnesium enhances the material's toughness and fracture resistance, making it well-suited for the demanding environment within the human body. Additionally, Mg-PSZ exhibits excellent wear resistance, which is crucial for the longevity and durability of implants. Its biocompatibility ensures that it integrates well with biological tissues, minimizing the risk of adverse reactions. These qualities make Mg-PSZ an attractive choice for a variety of medical implant applications, including dental, orthopedic, and spinal implants. Yusuf *et al.* have synthesized nano Mg-PSZ ceramic. The hardness of Mg-PSZ increases significantly from 554 MPa for undoped ZrO_2 to 5266 MPa with 10% MgO. *In-vitro* biodegradation tests demonstrate that higher concentrations of MgO doping in ZrO_2 lead to increased degradation resistance of Mg-PSZ in simulated body fluid (SBF) solution (Yusuf *et al.*, 2023). Sharifi *et al.* have prepared magnesia-partially stabilized zirconia (Mg-PSZ) discs and hydroxylated using a hydrothermal process at 120°C for varying durations to introduce reactive hydroxyl groups. Subsequently, these discs undergo immersion in a 0.01 mg/mL aqueous L-Serine solution at temperatures ranging from 40°C to 80°C and different pH conditions to graft L-Serine molecules onto the zirconia surface. Following this, the specimens are immersed in simulated body fluid (SBF) for 7 and 21 days. The findings reveal that grafting L-Serine on the zirconia surface at 80°C and neutral pH resulted in the creation of negative charges. Hydroxyapatite nucleation begins on the surfaces grafted with L-Serine

almost concurrently after 7 days of exposure to alkaline pH. The soaking is continued for 21 days, leading to the formation of more uniformly distributed mineral apatite with enhanced surface wettability (contact angle of 18.3° ± 1.3) (Sharifi *et al.*, 2024). Rahaman *et al.* have aimed to enhance the bioactivity and bone-bonding capability of magnesia partially stabilized zirconia (Mg-PSZ) orthopedic implants through coating with bioactive glass. Two silicate-based glasses (13–93 and 6P68) and one borosilicate glass (H12) are tested. The 6P68 glass exhibits the highest adhesive strength (40 ± 2 MPa) but demonstrates limited bioactivity. Conversely, the H12 glass shows lower adhesive strength (18 ± 2 MPa) but the highest bioactivity. To achieve a balance, a functionally graded coating is developed, comprising a 6P68 interfacial layer and an H12 surface layer, aiming to combine high adhesive strength with rapid in vitro bioactivity (Rahaman *et al.*, 2008). Cortés-Hernández *et al.* have developed bioactive Mg-PSZ composites by incorporating wollastonite ceramics either as part of the composite formulation or as a biomimetic treatment bed in simulated body fluids. Additionally, wollastonite-containing zirconia/alumina composites are also fabricated. The composites are immersed in SBF for 7 days with and without a bed of wollastonite powder, followed by re-immersion in 1.5 SBF for another 7 days. Mg-PSZ/$CaSiO_3$ and Mg-PSZ/Al_2O_3 composites exhibit highly bioactive surfaces. A uniform apatite layer is observed on Mg-PSZ/$CaSiO_3$ composites after just 7 days of immersion in SBF. In contrast, no apatite formation is detected on the Mg-PSZ/Al_2O_3/$CaSiO_3$ composite. During the sintering process, small amounts of aluminosilicate phases are formed and hindered apatite formation in the latter composite (Cortés-Hernández *et al.*, 2006).

2.8.3 Zirconia-toughened alumina (ZTA)

Zirconia-toughened alumina (ZTA) based bioceramics have garnered significant attention in the field of medical implants due to their exceptional combination of mechanical

and biological properties. Suh *et al.* have considered zirconia for use as an implant material. To address issues observed with hydroxyapatite (HA) coating on titanium implants, various methods have been proposed. These include HA-zirconia composite materials, HA-coated zirconia, and HA-zirconia functionally graded materials (FGM) or incorporating an intermediate alumina layer. These methods have demonstrated enhanced bonding strength and biocompatibility compared to traditional HA coatings on titanium implants, which are prone to low bonding strength and HA degradation (Suh *et al.*, 2019). Pezzotti *et al.* have modified the surface of zirconia-toughened alumina (ZTA) using two approaches: (i) laser patterning followed by filling patterned wells with powder mixtures of bioglass and Si_3N_4; and (ii) coating with Si_3N_4 using pulse-laser sintering. Both methods lead to osteoblast activation, a crucial factor for osteosynthesis applications (Pezzotti *et al.*, 2019). Pobloth *et al.* have evaluated four different coatings of varying thickness on zirconia toughened alumina (ZTA) ceramic implants to assess their osseointegration in a drill-hole model in sheep. The bioactive coatings include a layer of covalently bound multi-phosphonate molecules (CM), a nano-hydroxyapatite coating, and two different bioactive glass (BG) coatings of micrometer thickness: dip-coated 45S5 (DipBG) and sol-gel 70S30C (SGBG), which form a hydroxyl-carbonate apatite layer on the implant surface *in-vivo*. After 12 weeks, osseointegration is assessed through mechanical push-out testing and histological analysis. Results show that the nano-hydroxyapatite coating significantly enhances maximum push-out force, adhesive shear strength, and energy release rate. Additionally, CM coating increases the implant-bone interfacial stiffness (Pobloth *et al.*, 2019). Ponnilavan *et al.* have explored the structural and bioactive characteristics of alumina-zirconia composite (AZC) by the addition of Ca^{+2} and PO_4^{3-} ions. Immersion tests in simulated body fluid (SBF) confirm the enhanced bio-mineralization activity of AZC due to the presence of Ca^{2+} and PO_4^{3-} ions. Indentation tests demonstrate consistent elastic modulus and hardness across all investigated specimens. Moreover, *in-vitro* cell culture

experiments confirm the bioactivity of all AZC compositions (Ponnilavan *et al.*, 2019). Esfahani *et al.* have investigated the bioactivity and cytocompatibility of an electrospun polyamide 6(PA6)/hydroxyapatite (HA) coating applied onto zirconia-toughened alumina (ZTA) ceramics. By adjusting the PA6/HA ratio to 1.15 (w/w), an effective fibrous coating with an average diameter of 120 ± 10 nm and surface porosity of 64.3% is achieved. Both bare and coated samples exhibit hydrophilic surfaces conducive to bone regeneration. *In-vitro* bioactivity tests are conducted in simulated body fluid (SBF) confirming the formation of a nanostructured bonelike apatite phase on the PA6/HA coating. Cytocompatibility assessments using MG63 osteosarcoma-like cells demonstrate that the electrospun PA6/HA coating significantly enhances cell attachment and spreading (Esfahani *et al.*, 2018). Zhang *et al.* have aimed to examine how the inclusion of zirconia nanoparticles affects the microstructure and mechanical properties of glass-infiltrated alumina/zirconia composites (AZGs). Various slip-cast zirconia-toughened alumina (ZTA) compacts containing 10%, 20%, and 30% nano-zirconia by weight are partially sintered and subsequently infiltrated with lanthanum borosilicate glass of lower thermal expansion. The partially sintered ZTA samples exhibit porosity levels ranging from 21% to 25%, predominantly with submicron-sized pores. The mechanical strength and fracture toughness of the AZGs are increased with the zirconia content. The highest values (633.5 ± 41.7 MPa and 6.7 ± 0.6 MPa·m^0.5) are observed with 30% nano-zirconia and attributed due to the higher zirconia content and the presence of thinner intergranular glass film (Zhang *et al.*, 2012).

2.9 Machinability study of zirconia-based bioceramics composites

Machinability refers to the ease with which a material can be machined to meet the desired dimensions, surface finish, and shape using conventional machining processes like turning, milling, drilling, and grinding. Machinability is a critical factor in the manufacturing

and application of bioceramics when these materials are used in medical implants. Paper was successfully sliced with a low-pressure water jet device that was patented in the 1930s. (Charles *et al.*, 1933). Twenty years later, water jet machining introduced a high-pressure hydraulic seal from the aviation industry, which significantly improved process productivity (Schwacha *et al.*, 1958). Over the ensuing decades, the operating pressure was steadily increased, making it possible to cut through resistant metals and carbides. However, excessive pressure caused a great deal of nozzle wear, rendering abrasive jet machining (AJM) economically unviable. Abrasive jet systems were first commercially accessible in the 1970s following the introduction of ceramic nozzles. It quickly became the industrial standard and was mostly used for cutting and cleaning. The development of AJM veered off course toward technology miniaturization in the twenty-first century, resulting in a drop in nozzle diameter from macro to micro scale. Even though AJM has been in use for a century, modern sapphire orifice, ultra-hard abrasives, dependable high-pressure pumps, and 6-axis, precisely controlled and process monitoring systems make it one of the most promising micro-manufacturing methods. Over the past two decades, there has been a consistent increase in corporate interest in micro-AJM. A high volume of research activity is a clear indicator of the demands of the industry.

Various manuscripts (Chen *et al.*, 2017) (Verma *et al.*, 2014) (Syazwani *et al.*, 2016) (Molitoris *et al.*, 2016) (Kalpana *et al.*, 2015) have provided the latest technological state of AJM. Nevertheless, Chen *et al.* have focused on the polishing capabilities of AJM (Chen *et al.*, 2017). Verma *et al.* and Syazwani *et al.* have reviewed the nozzle wear in abrasive water jet machining (AWJM), separately (Verma *et al.*, 2014) (Syazwani *et al.*, 2016). Molitoris *et al.* have reported on the developments of abrasive water suspension jets (Molitoris *et al.*, 2016). Kalpana *et al.* have analyzed only the process monitoring methods (Kalpana *et al.*, 2015). In light of this research, it is imperative to close the gaps and present a thorough

overview of the state of the art in abrasive jet machining (AJM), covering its technological advantages and disadvantages, an examination of AJM advancements and material removal mechanisms, the impact of process variables on surface integrity, texturing capabilities, and nozzle wear. Banerjee *et al.* have worked to use ultrasonic micromachining (USMM) to maximize the quality of micro-hole formation in zirconia ceramic. This study considers three important process variables: the concentration of the abrasive slurry, the tool feed rate, and the power rating. Responses include the overcut, taper angle, and material removal rate. Through the process of multi-objective optimization, a power rating of 386.87 W, a slurry concentration of 49.59% g/l, and a tool feed rate of 1.16 mm/min is determined. Within these parameter settings, the machining of ZrO_2 ceramics results in a maximum MRR of 0.5333 mm^3/min, a minimum taper angle of 0.3428 degrees, and a minimum overcut of 36.64 µm (Banerjee *et al.*, 2024). Samantaray *et al.* have compared the sustainability and performance of classic AJM of zirconia ceramic to newly invented hot abrasive jet machining (hot-AJM). The modified AJM strikes on the work surface for material erosion using an abrasive air jet (a mixture of hot abrasive and compressed air). The investigation of cutting performance involves a comparison of technological parameters, specifically material removal rate, machining cost, and vibration of the machine tool. The process variables for machining trials include abrasive grain size, nozzle pressure, and stand-off distance. According to the findings, the hot-AJM performed better than the standard AJM in terms of enhanced material removal, decreased vibration, and low machining costs (Samantaray *et al.*, 2024). Balasubramaniyan *et al.* have investigated how the desirable machining responses, such as surface roughness (Ra) and kerf taper (KT), are affected in AWJM machining experiments by machining parameters such as abrasive flow rate, water jet pressure, and nozzle traverse speed (Balasubramaniyan *et al.*, 2024). Balamurugan *et al.* have created a novel ceramic matrix composite with proportionate concentrations of yttria (Y_2O_3) (20 wt.%) and lanthanum

phosphate ($LaPO_4$) (80 wt.%). Abrasive water jet machining is used to machine the prepared ceramic matrix composite (AWJM). To quantify variances in performance characteristics such as material removal rate (MRR), kerf angle (KA), and surface roughness (Ra), grey relational analysis (GRA) is conducted with a variety of input factors including jet pressure (JP), stand-off distance (SOD), and traverse speed (TS). It is clear from the experimental study that SOD significantly influences the output performance characteristics, accounting for roughly 60.89% of the total (Balamurugan *et al.*, 2018). Chakravarty *et al.* have investigated the mechanical characteristics and microstructure of composites created by spark plasma sintering (SPS) and the impact of the addition of nanocrystalline ZrO_2 and TiCN to ultrafine Al_2O_3. The machining performance of nanocomposite inserts is enhanced by their increased toughness, even at high cutting speeds of ≥500 m min^{-1} (Chakravarty *et al.*, 2013). Abdo *et al.* have generated micro-channels on zirconium oxide (ZrO_2) using rotary ultrasonic machining (RUM). The impacts of critical RUM input parameters, such as cutting speed (S), feed rate (FR), depth of cut (DOC), frequency (F), and amplitude (A), on the surface roughness (Ra), edge chipping (EC), depth error (DE), and width error (WE) of the milled micro-channels are investigated using a full factorial design of experiments. To find the ideal parametric parameters for minimizing the values of Ra, EC, DE, and WE of the created microchannels, the multi-objective genetic algorithm (MOGA) is utilized. The results show that the multi-objective optimization at higher frequencies and amplitudes and lower feed rates, depth of cut, and cutting speeds may achieve the minimal values of Ra = 0.26 μm, EC = 10.1 μm, DE = 4.2%, and WE = 7.2% (Abdo *et al.*, 2020).

2.10 Tribological study of zirconia-based bioceramic composites

Tribology encompasses the study of friction, wear, and lubrication. The tribological study of zirconia-based bioceramic composites is crucial for optimizing their performance in

biomedical applications. By understanding the wear mechanisms and factors affecting tribological behavior, researchers can develop more durable and reliable implants. Ongoing research in material modifications and surface engineering continues to enhance the properties of zirconia composites, making them even more suitable for a wide range of biomedical applications. Alghauli *et al.* have concurrently improved the mechanical and tribological capabilities, as well as the forming accuracy, of translucent glass-ceramics. A method for adding Al_2O_3 whiskers is presented. The outcomes show that fluorapatite (FAp) glass-ceramics' forming accuracy, mechanical, and tribological capabilities are greatly enhanced by the addition of Al_2O_3 whiskers. In comparison to pure FAp glass-ceramics, the glass-ceramics with 10 weight percent Al_2O_3 whiskers show a higher flexural strength and fracture toughness of 220.3±13.7 MPa and 1.81±0.18 MPa•$m^{1/2}$, respectively. Additionally, the inclusion of Al_2O_3 whiskers results in a decrease in wear volume in the titanium and glass-ceramic balls that serve as equivalents, demonstrating enhanced tribological compatibility (Alghauli *et al.*, 2014). Faria *et al.* have made green zirconia compacts by cold pressing, then surface texturing using a ns-Nd: YAG laser and sintering in a high-temperature furnace to complete the functionalization process. Subsequently, the textured surfaces undergo a 45S5 bioglass coating via a dip-coating process, which is subsequently sintered via CO_2 laser. Biaxial flexural tests are performed to evaluate the mechanical resistance of zirconia. The results show a flexural strength value (520 ± 65 MPa) that meets ISO 13356:2008 criteria. The outcomes demonstrate that a potential method for creating zirconia-based implants with the increased bioactivity needed for successful osseointegration appears to be the synergistic effect of combined physical and chemical modifications (Faria *et al.*, 2022). Smirnov *et al.* have used laser surface texturing to enhance the antibacterial and tribological performance of 3Y-TZP ceramics. The findings show that adding microtextures can alter the zirconia surface's solid-liquid interface, which in turn can alter how wettable it

is. One important aspect that determines the antibacterial activity of textured zirconia ceramics is wettability. A hydrophobic surface performs better against bacteria because it is better at preventing their adherence, extension, and reproduction. The zirconia ceramics' wear resistance is improved, albeit their effectiveness is reliant on the structural strength and density of the texture. The outcomes can offer technological direction for the development and use of microtextures in the fields of restorative dentistry (Smirnov *et al.*, 2018). Rodríguez-Rojas *et al.* have investigated the dry sliding-wear response of a ZrO_2-doped 3Y-TZP monolithic and of two 3Y-TZP composites. The composites are reinforced with either 1-D carbon nanofibres (CNFs) or 2-D reduced graphene oxide (rGO) nanoplatelets and evaluated by ball-on-disk tests at moderate load, and compared critically. According to the findings, 3Y-TZP, 3Y-TZP/CNFs, and 3Y-TZP/rGO all composites experience minor wear due to abrasion, with contributions from fracture and plastic deformation. The presence or absence of self-lubricating tribofilms on the contact surface correlates with wear resistance rather than toughness or hardness. In particular, 2-D rGO nano-reinforcements pull out and provide a solid-state lubrication that lowers the coefficient of friction (CoF), giving 3Y-TZP/rGO more wear resistance than 3Y-TZP and 3Y-TZP/CNFs. Nevertheless, 1-D CNF nano-reinforcements hardly ever produce these tribofilms, therefore they have little impact on wear resistance and the CoF. The dimensionality of the carbon-based nano-reinforcements and the testing parameters that affect the microstructural design of ceramic composites for tribological applications are also explored (Rodríguez-Rojas *et al.*, 2021). Golieskardi *et al.* have created stable zirconia ceramics doped with Al_2O_3 and CeO_2 using a widely accessible, reasonably priced sintering method. Comparing Al_2O_3 and CeO_2-doped 3Y-TZP samples to undoped 3Y-TZP samples, it is found that the volumetric wear and roughness values are much reduced. Over the course of 24 weeks, submerging the samples in Ringer's solution at 37°C reveals low-temperature deterioration resistance. The degradation patterns suggest that

the use of dopants is advantageous from a technical standpoint when it comes to the aging of ceramic samples (Golieskardi *et al.*, 2020). Huang *et al.* have demonstrated the advantages of a small amount of CaF_2 (1 wt%) as a solid lubricant in magnesium oxide (MgO) doped 3Y-TZP composites. Due to the presence of a smooth tribo layer at the contacting surfaces, the addition of 0.5 weight percent MgO to the ceramic composite results in a decrease in the mean coefficient of friction (μ) to approximately 42% and a subsequent wear rate (k) to approximately 31% as compared to pure 3Y-TZP (Huang *et al.*, 2019). Mazumder *et al.* have examined the impact of mullite content on the microstructure and tribological properties of in-situ mullite-toughened 3Y-TZP ceramics. The wear rate and coefficient of friction of the sample containing 4 mol% mullite are significantly reduced. The overall structure of the samples containing 6, 8, and 10 mol% mullite are severely damaged by a high proportion of irregular mullite, and this, along with high porosity, not only decreases the samples' mechanical properties but also increases surface roughness, which drastically decreased the material's resistance to wear (Mazumder *et al.*, 2019). Buciumeanu *et. al.* have assessed the tribological performance of bioactive zirconia composite layers applied to yttria-stabilized zirconia (YSZ) substrates. There are two varieties, reinforced with 10% HAp and 10% β-TCP, of bioactive zirconia composite layers examined. The findings show that the addition of bioactive ingredients does not affect the tribological performance. There is no variation in the coefficient of friction across all samples, and the particular wear rates are all within the same order of magnitude. These findings demonstrate the potential of this novel strategy, which employs a bioactive zirconia composite layer on a zirconia substrate to preserve the high tribological qualities while simultaneously strengthening the bond between the implant and living tissue (Buciumeanu *et al.*, 2018). Smirnov *et al.* have evaluated the tribological behavior of 3Y-TZP monolithic ceramic and 3Y-TZP/Ta (20 vol%) ceramic-metal composites. The ultra-high-molecular-weight polyethylene (UHMWPE)–3Y-TZP/Ta system

demonstrates a lower volume loss and friction coefficient than the UHMWPE–monolithic ceramic combination, as per the results of the pin (UHMWPE)-on-flat wear test conducted in dry conditions. Compared to the UHMWPE-zirconia monolithic material, it is found that aging has less impact on the wear characteristics of the UHMWPE-biocomposite system. 3Y-TZP/Ta composites demonstrate strong resistance to low-temperature deterioration and favorable tribological characteristics, indicating their potential for use in biomedical applications, particularly in the field of orthopaedic implants (Smirnov *et al.*, 2022). Santos *et. al.* have studied the tribological behavior of a dental glass-ceramic (GC) reinforced with 20% (vol.) yttria-stabilized zirconia. Pre-sintered zirconia particles (ZP) and zirconia agglomerates (ZA) are the two types of particles that are evaluated. The outcomes show that the wear behavior of GC is enhanced by ZP. ZP-reinforced dental glass ceramics may be a viable substitute for traditional glass ceramics in the production of prosthetic restorations (Santos *et al.*, 2016).

2.11 Summary of literature review

The literature review suggests that several researchers have developed modified bioceramic materials for biomedical applications. The summary of the literature review is given as follows:

- After a literature survey, it is found that nowadays 3Y-TZP, 8Mg-PSZ, and ZTA ceramics are used in the biomedical field due to their excellent mechanical and biocompatibility properties. However, its application is restricted because 3Y-TZP, 8Mg-PSZ, and ZTA ceramics are bio-inert materials.
- To make bioactive from bio-inert, different techniques are used like coating, chemical treatment, and incorporation of bioactive materials like BG, HA, $CaPO_4$, etc.

- Different types of bioactive glasses are used as biomaterials like 45S5, 13-93 BG, 58S, etc. In comparison to 45S5 & 58S, 13-93 BG have additional functional groups like K_2O and MgO, which affect the reaction kinetics.
- There is very limited research on the impact of incorporating bioactive glass on the mechanical properties, such as flexural strength, compressive strength, hardness, and elastic moduli, of bioceramic composites based on 3Y-TZP, 8Mg-PSZ, and ZTA.
- The effect of adding bioactive glass on the machinability of 3Y-TZP-based composites has not been studied to date. Machinability is a crucial characteristic of implant materials, as implants must be processed into specific shapes and sizes to match patient geometry.
- There is very limited research on the influence of bioactive glass addition on the tribological behavior of 3Y-TZP-based composites. Load-bearing implants, such as those used in hips, knees, and dental procedures, endure mechanical loads and create frictional pairs, leading to material degradation. Therefore, it is essential to study the tribological behavior of these composites.

2.12 Research objectives

The primary objective of this research is to create a bioactive bioceramic composite from bio-inert ceramic, enhancing its in-vitro bioactivity, cellular viability, and antibacterial response by incorporating bioactive glass. Additionally, the study explores the effect of bioactive glass addition on the machinability, mechanical, and tribological behavior of optimized bioceramic composite systems. Fig. 2.3 shows the schematic representation of the overall research objectives of the present work. To achieve these goals, the research is divided into the following specific objectives:

(a) To synthesize 3Y-TZP, 8Mg-PSZ, and ZTA bioceramics for matrix and 13-93 BG for reinforcement.

(b) To fabricate bio-ceramic composites by varying amounts (0–25 wt.%) of bioceramics with 13-93 BG and optimize the processing parameters.

(c) To examine the phases, microstructure, mechanical, *in-vitro* bioactivity, cellular viability, and the antibacterial response of 3Y-TZP/13-93 BG bioceramic composites.

(d) To study the phases, microstructure, mechanical, *in-vitro* bioactivity, cellular viability, and the antibacterial response of 8Mg-PSZ/13-93BG bioceramic composites.

(e) To analyse the phases, microstructure, mechanical, *in-vitro* bioactivity, cellular viability, and the antibacterial response of ZTA/13-93BG bioceramic composites.

(f) To investigate the influence of 13-93 BG addition on the machinability of the optimized (3Y-TZP /13-93BG) composites.

(g) To explore the influence of 13-93 BG addition on the tribological response of the optimized (3Y-TZP /13-93BG) composites.

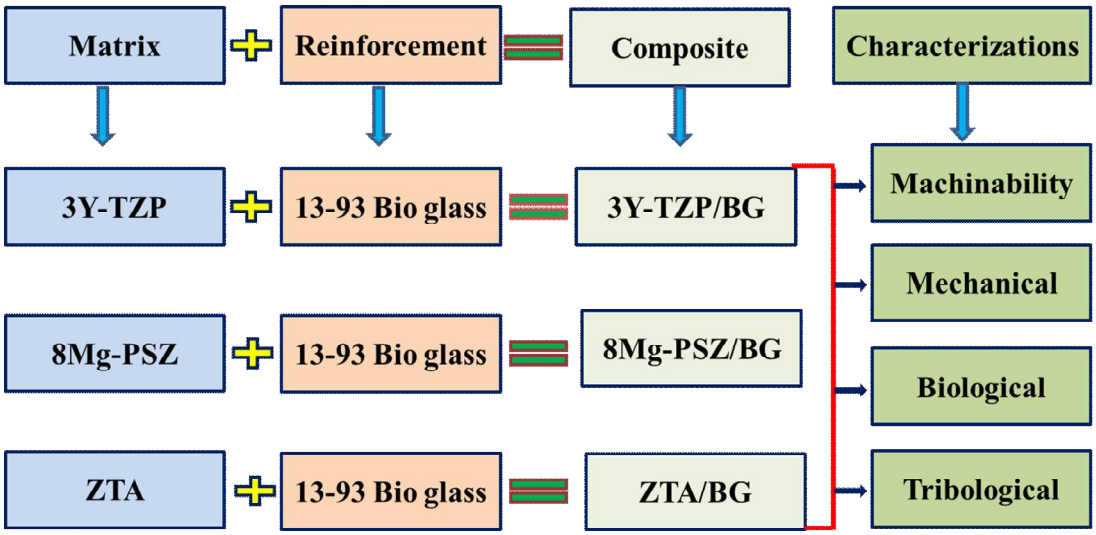

Fig. 2.3 Schematic representation of overall research objectives of the present work.